Design of Marx generators as a structured eigenvalue assignment

Sergio Galeani[1], Didier Henrion[2,3], Alain Jacquemard[4,5], Luca Zaccarian[2,6]

August 2, 2013

Abstract

We consider the design problem for a Marx generator electrical network, a pulsed power generator. The engineering specification of the design is that a suitable resonance condition is satisfied by the circuit so that the energy initially stored in a number of storage capacitors is transferred in finite time to a single load capacitor which can then store the total energy and deliver the pulse. We show that the components design can be conveniently cast as a structured real eigenvalue assignment with significantly lower dimension than the state size of the Marx circuit. Then we comment on the nontrivial nature of this structured real eigenvalue assignment problem and present two possible approaches to determine its solutions. A first symbolic approach consists in the use of Gröbner basis representations, which allows us to compute all the (finitely many) solutions. A second approach is based on convexification of a nonconvex optimization problem with polynomial constraints. We show that the symbolic method easily provides solutions for networks up to six stages while the numerical method can reach up to seven and eight stages. We also comment on the conjecture that for any number of stages the problem has finitely many solutions, which is a necessary assumption for the proposed methods to converge. We regard the proof of this conjecture as an interesting challenge of general interest in the real algebraic geometry field.

1 Introduction

Electrical pulsed power generators have been studied from the 1920s with the goal to provide high power electrical pulses by way of suitable electrical schemes that are slowly charged and then, typically by the action of switches, are rapidly discharged to provide a high voltage impulse or a spark (see, e.g., [5]). Marx generators (see [5, §3.2] or [7]

[1]DICII, Università di Roma Tor Vergata, Italy.
[2]CNRS, LAAS, University of Toulouse, France.
[3]Faculty of Electrical Engineering, Czech Technical University in Prague, Czech Republic.
[4]CNRS, IMB, Université de Bourgogne, Dijon, France.
[5]Wolfgang Pauli Institut, Vienna, Austria.
[6]Dipartimento di Ingegneria Industriale, University of Trento, Italy

for an overview) were originally described by E. Marx in 1924 and correspond to circuits enabling generation of high voltage from lower voltage sources. While many schemes have been proposed over the years for Marx generators, a recent understanding of certain compact Marx generators structures [6] reveals that their essential behavior can be well described by a suitable LC ladder network where certain components should be designed in order to guarantee a suitable resonance condition. In turn, such a resonance condition is known to lead to a desirable energy transfer throughout the circuit and effective voltage multiplication which can then be used for pulsed power generation.

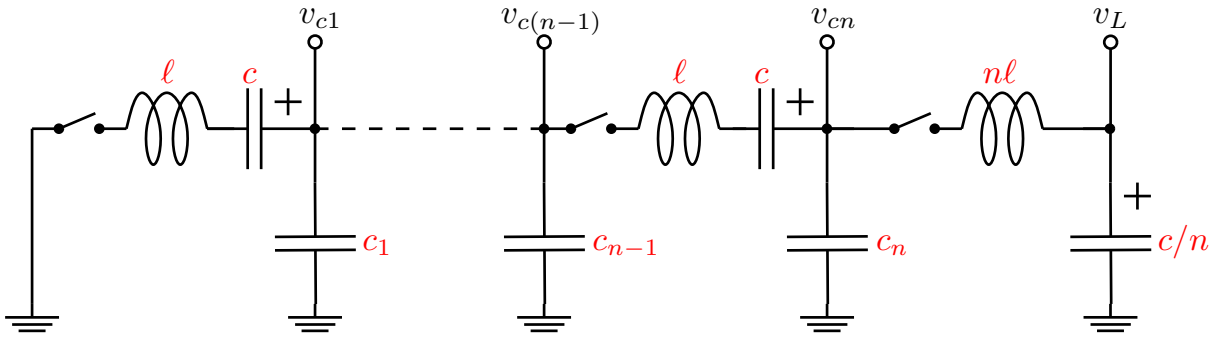

Figure 1: The passive circuit used as a Marx generator.

This paper addresses the mathematical problem of designing the lumped components of the compact Marx generator circuit well described in [6] and represented in Figure 1. In particular, in [6], based on a Laplace domain representation of the ladder network of Figure 1, several experimentally oriented discussions are provided illustrating that, as long as the vertical (parasitic) capacitors of the network are suitably selected to guarantee a certain resonance property, the network performs very desirably in terms of pulsed power generation. Despite its fundamental importance from the experimental viewpoint, [6] does not provide a viable technique for ensuring this resonance property and uses heuristics to find some solutions to the design problem for some fixed number of stages. A similar approach has been taken in the Master thesis [1], where a state-space description of the same circuit has been presented and a nonlinear least squares approach has been proposed to ensure the desirable resonance property. Both the works outlined above have followed heuristic approaches for the computation of the circuit components ensuring resonance. Conversely, in this paper we introduce a substantially different approach to the design problem by showing, via suitable transformations, that this design can be cast as a structured real eigenvalue assignment problem for a linear system associated with the Marx network of Figure 1 and only depending on the number of its stages.

The problem of static output feedback pole (or eigenvalue) assignment for linear systems has been largely studied in the 1990s, see [26] for a survey. In its simplest form, it can be stated as follows: given matrices $A \in \mathbb{R}^{n\times n}$, $B \in \mathbb{R}^{n\times m}$, $C \in \mathbb{R}^{p\times n}$ and a monic polynomial $q(s) \in \mathbb{R}[s]$ of degree n, find an $m \times p$ real matrix F such that $\det(sI_n - A - BFC) = q(s)$ where I_n denotes the identity matrix of size n. This problem has generically a solution if $mp > n$, and it has generically no solution if $mp < n$. The situation $mp = n$ is much more subtle. For this situation, it was proved in [12, 13] that the pole placement map from the feedback matrix F to the characteristic polynomial $q(s)$ is generically not surjective.

It means that there is a non-empty open subset of real matrices A,B,C for which there exist open sets of pole configurations symmetric w.r.t. the real axis which cannot be assigned by any real feedback. In this paper, we do not consider static output feedback pole assignment in the form just described, but in a structured form. The number of degrees of freedom (number of entries in the feedback matrix) is equal to n, the number of poles to be assigned, so it bears similarity with the difficult case $mp = n$ of static output feedback pole assignment described above.

Within the context of the above cited works [26, 12, 13], the structured pole assignment problem that we characterize in this paper corresponds to the case where $C = I_n$ and F is diagonal, which is a case not covered by these works. For this problem, we provide in this paper a few general results characterizing its solutions, and then show how one can tackle the solution. For computationally tractable cases, a first technique, based on Gröbner basis representations, allows determining the full set of solutions, or in other words all the possible selections of the circuit components leading to the desired energy transfer. A second numerical technique, based on nonconvex polynomial optimization tools, allows determining one solution which is optimal in the sense that it minimizes a certain polynomial cost function. In the paper we state assumptions requiring that the solution set is nonempty (that is, there exists at least one choice of the parameters leading to the desired resonance condition) and that the number of solutions is actually finite, namely the set of all solutions is a zero-dimensional set. These assumptions imply desirable termination and convergence properties of the symbolic and numerical techniques which are highlighted in the paper. Interestingly, numerical evidence reveals that these assumptions are satisfied for all the numerically tractable cases that have been considered, however their general validity is an interesting open problem. Additional work related to the techniques reported here corresponds to [8] and references therein, where algebraic techniques (elimination theory using resultants) are used in the design of power electronic devices. In this reference the authors show that parasitic higher order harmonics in a multilevel converter can be removed by solving a structured polynomial system of equations featuring a high degree of symmetry.

Preliminary results along the direction of this paper were presented in [35], where Laplace domain descriptions were used and where a result roughly corresponding to one of the key components of our proof (that is, Lemma 3 in Section 5.2) was stated without any proof. Here, in addition to proving that result, we provide a more complete statement establishing sufficient conditions for the desired pulsed power generation. Moreover, we adopt a state-space representation that allows to provide a very elegant and compact proof of our main result. Finally, an important contribution of this paper consists in the two solution methods outlined above. The symbolic one allows us to enumerate all the possible components selections ensuring the resonant conditions for circuits with up to $n = 6$ stages. The numerical one allows us to compute the so-called "regular solution" (characterized in Section 3.2) for the more convoluted cases $n = 7$ and $n = 8$. While typical experimental realizations of the Marx generator of Figure 1 does not involve a larger number of stages, the problem of solving the presented structured eigevnalue problem for larger values of n constitutes an interesting benchmark problem for researchers in the algebraic geometric field.

The contributions of this paper consist in the following three points: A) establishing suf-

ficient conditions for the energy transfer goal behind the architecture of Figure 1 (the problem statement and main results are presented in Section 2 and the proofs are reported in Section 5). B) illustrating two methods to solve those conditions: a symbolic one, treated in Section 3, and a numerical one, treated in Section 4. Both methods are of interest for the addressed experimental problem due to suitable trade-offs between complexity and achievable results; C) illustration of the potential behind the adopted Gröbner basis representation and the adopted numerical optimization of convex relaxations by way of suitable "engineering-style" propositions establishing the applicability limits of thsoe two approaches. Finally, some discussions about the above mentioned conjectures and the relevance of this study as a challenge within the algebraic geometric field are given in Section 6, while Appendix 6 contains some illustrative smaple Maple code implementing our algorithms.

Notation: Given a square matrix A, $\sigma(A)$ denotes its spectrum, i.e., the set of its complex eigenvalues. Given a vector $f \in \mathbb{R}^n$, $\mathbb{Q}[f]$ denotes the set of all polynomials with rational coefficients in the indeterminates f.

2 Marx generator design

2.1 Circuit description and problem statement

We consider the Marx generator network shown in Figure 1 consisting in n stages (and $n+1$ loops) where, disregarding the two rightmost components of the figure, each one of the n stages consists in 1) an upper branch with a capacitor and an inductor and 2) a vertical branch with a capacitor only. Following [1, 35, 6], we assume that all the capacitors and inductors appearing in the upper branches are the same (corresponding to some fixed positive reals c and ℓ). We will call these capacitors "storage capacitors" in the sequel, for reasons that will become clear next. The design problem addressed here is the selection of the vertical capacitors, which are exactly n, where n is the number of stages of the Marx circuit. We will call these capacitors "parasitic capacitors" due to their position resembling that of parasitic capacitors in transmission lines. Despite their name, the parasitic capacitors c_i, $i = 1, \ldots, n$ are not necessarily arising from any parasitic effects and their values will be selected in such a way to ensure a suitable resonance condition as clarified next.

Following [1, 35, 6], the inductance and capacitor appearing in the rightmost loop take the values $n\ell$ and c/n, respectively. We call this capacitor the "load capacitor". This selection preserves the resonance property (so that the product of any adjacent capacitor/inductor pairs is always ℓc) in addition to ensuring that the load capacitor is n times larger than each one of the storage capacitors. The problem addressed in this paper (resembling that one tackled in [1, 35, 6]) is the following.

Problem 1 *Consider the circuit in Figure 1 for given n and certain values of c and ℓ. Select positive values $c_i > 0$, $i = 1, \ldots n$ of the parasitic capacitors and a time $T > 0$ such that, initializing at $t = 0$ all the storage capacitors with the same voltage $v(0) = v_\circ$ and starting from zero current in all the inductors and zero voltage across the parasitic*

capacitors and the load capacitor, the circuit response is such that at $t = T$ all voltages and currents are zero except for the voltage across the load capacitor.

Remark 1 The resonance condition required in Problem 1 is a key feature to allow the use of the circuit of Figure 1 for pulsed power generation. In particular, assuming that a number of switches are used to open the loops of the circuit, the n storage capacitors can be charged at the same voltage $v_\circ$. Due to the property in Problem 1, at time T, all the energy initially stored in the storage capacitors will be concentrated in the load capacitor. In particular, since this is a lossless circuit, we will have

$$\sum_{i=1}^{n} \frac{1}{2} c v_\circ^2 = \frac{1}{2} \frac{c}{n} v_L^2(T),$$

which clearly implies $v_L(T) = n v_\circ$, namely both the voltage and energy transferred to the load capacitor is n times larger than the voltage and energy initially stored in each one of the storage capacitors. ∘

2.2 Solution via structured eigenvalue assignment

In this section we show that a solution to Problem 1 can be determined from the solution of a suitable structured eigenvalue assignment problem involving a matrix $B \in \mathbb{R}^{n \times n}$ defined as

$$B := \begin{bmatrix} 2 & -1 & 0 & \cdots & 0 \\ -1 & \ddots & \ddots & \ddots & \vdots \\ 0 & \ddots & \ddots & \ddots & 0 \\ \vdots & \ddots & \ddots & 2 & -1 \\ 0 & \cdots & 0 & -1 & \frac{n+1}{n} \end{bmatrix} \tag{1}$$

and an arbitrary set of even harmonics of the fundamental frequency $\omega_0 = \sqrt{(\ell c)^{-1}}$ to be assigned to the circuit. The following is the main result of this paper, whose proof is given in Section 5.

Theorem 1 *Consider any set of n distinct positive even integers $\alpha = (\alpha_1, \ldots, \alpha_n)$, the matrix B in (1) and any positive definite real diagonal solution $F = \mathrm{diag}(f_1, \ldots, f_n)$ to the structured eigenvalue assignment problem*

$$\sigma(BF) = \{\alpha_1^2 - 1, \ldots, \alpha_n^2 - 1\}. \tag{2}$$

Then for any value of c, the selection $c_i = c/f_i$, $i = 1, \ldots, n$, solves Problem 1 for all values of ℓ with $T = \frac{\pi}{\sqrt{\ell c}}$.

Theorem 1 shows that a solution to Problem 1 can be determined by solving an eigenvalue assignment problem with decentralized feedback (because matrix F is diagonal). Note that this structured eigenvalue assignment problem arises naturally from the physical nature of the circuit under consideration and does not arise from some simplifying

assumptions on the circuit behavior. A generalized version of this structured pole assignment problem was studied in [34] (indeed, using the notations there, the pole assignment problem in (2) is obtained by setting $r = n$, $C = I_n$, $m_i = p_i = 1$, $i = 1, \ldots, n$). It is shown in [34] that generic pole assignment depends on the dimension of a product Grassmannian, see [34, Equ. (17)]. In our case it is equal to $n!$ which is always even, and from [34, Theorem 4.2] it follows that generic pole assignment cannot be achieved. A geometric condition that ensures generic pole assignment is given in [34, Prop. 4.2] but we do not know whether this condition can be checked computationally. In any case it is an evidence that the question of existence of a real solution to our inverse eigenvalue problem does not appear to be trivial.

Remark 2 Bearing in mind that F is diagonal, real and positive definite, the inverse eigenvalue problem (2) can be equivalently cast as a symmetric inverse Jacobi eigenvalue problem (IJEP) (see, e.g., [9, 10]) by performing the coordinate change with $T = \sqrt{F}$, which leads to

$$M := T(BF)T^{-1} = \sqrt{F}B\sqrt{F}, \tag{3}$$

where it is evident that $M = M^T > 0$. In particular, positive definiteness of M arises from positive definiteness of B which is established in the proof of Lemma 3. Since (3) is a change of coordinates, then assigning the spectrum $\{\alpha_1^2 - 1, \ldots, \alpha_n^2 - 1\}$ to the matrix M is equivalent to solving the eigenvalue assignment problem (2) with the possible advantage that M is a symmetric matrix. ∘

The following result shows that any solution to (2) is physically implementable as it corresponds to positive values of the parasitic capacitors.

Lemma 1 *Any solution to the structured eigenvalue assignment problem (2) in Theorem 1 is such that $F > 0$.*

Proof. Given any solution to (2), all the diagonal entries of F are necessarily nonzero otherwise BF would be rank deficient which contradicts the fact that $\sigma(BF)$ only has strictly positive elements. Define $F = \bar{F}D$, where $\bar{F} > 0$ is diagonal and D is a diagonal matrix whose elements are either 1 or -1.

Assume now that the statement of the proposition is not true so that D has at least one negative entry. We consider the coordinate transformation $\sqrt{\bar{F}}BF\sqrt{\bar{F}}^{-1} = \sqrt{\bar{F}}B\sqrt{\bar{F}}D =: \bar{M}D$, where the last equality follows from the fact that $\bar{F}$ and D are both diagonal. Due to the coordinate transformation, all the eigenvalues of $\bar{M}D$ are positive (because they are the same as those of BF). Since $B > 0$ (see the proof of Lemma 3 in Section 5.2) we have that $\bar{M} := \sqrt{\bar{F}}B\sqrt{\bar{F}}$ is symmetric positive definite, so that there exists an orthogonal matrix Q such that $\bar{M} = Q\Lambda Q^T$, with Λ diagonal positive definite. Then it follows that $Q^T\bar{M}D = \Lambda Q^T D$ which, pre-multiplied by $(\sqrt{\Lambda})^{-1}$ and post-multiplied by $Q\sqrt{\Lambda}$ leads to

$$\Sigma := (\sqrt{\Lambda})^{-1}Q^T\bar{M}DQ\sqrt{\Lambda} = \sqrt{\Lambda}Q^T DQ\sqrt{\Lambda},$$

which establishes that the matrix Σ is symmetric (rightmost term) and has positive eigenvalues (middle term which is a coordinate transformation from BF). Nevertheless, the matrix D is not positive definite by assumption, which leads to a contradiction. □

2.3 Two equivalent eigenvalue assignment formulations

Selecting the diagonal entries $f = [f_1 \cdots f_n]^T$ to solve the eigenvalue assignment (2) amounts to solving a finite set of n equations (polynomial in the unknown f with rational coefficients), each of them corresponding to one coefficient of the following polynomial identity in the variable s:

$$\det(sI - BF) = \prod_{i=1}^{n} \Big(s - (\alpha_i^2 - 1)\Big), \quad \forall s \in \mathbb{C}. \tag{4}$$

As an example, for the case $n = 2$, where $BF = \left[\begin{smallmatrix} 2f_1 & -f_1 \\ -f_2 & \frac{3}{2}f_2 \end{smallmatrix}\right]$, if one makes the simple [1] selection $\alpha = (2, 4)$, then the set of polynomial equations ensuring (4) corresponds to:

$$\left\{ \begin{array}{rcl} 2f_1 f_2 & = & (\alpha_1^2 - 1)(\alpha_2^2 - 1) = 45 \\ 2f_1 + \frac{3}{2}f_2 & = & (\alpha_1^2 - 1) + (\alpha_2^2 - 1) = 18. \end{array} \right. \tag{5}$$

In the general case, for a fixed value of n and fixed values in α, one can write a system of n polynomial equations in the variable f with rational coefficients, namely

$$p_i(f) = 0, \quad i = 1, \ldots, n. \tag{6}$$

In this paper, we will also adopt an alternative formulation of the problem which appears to be more suitable for the numerical optimization techniques developed in Section 4. The alternative formulation corresponds to inverting the eigenvalue assignment problem (2), thereby obtaining an alternative set of polynomial equations in the unknowns $k = [k_1 \cdots k_n]^T = [f_1^{-1} \cdots f_n^{-1}]^T$ with rational coefficients, which have the advantage of being linear in the capacitor values, indeed, $k_i = c_i/c$, $i = 1, \ldots, n$. In particular, for the inverse problem, equation (4) becomes

$$\det(sI - KB^{-1}) = \prod_{i=1}^{n} \Big(s - (\alpha_i^2 - 1)^{-1}\Big), \quad \forall s \in \mathbb{C}, \tag{7}$$

where $K = \mathrm{diag}(k) = F^{-1}$ is a diagonal matrix whose diagonal elements are the scalars to be determined. Similar to above, for the case $n = 2$, we have $KB^{-1} = \left[\begin{smallmatrix} \frac{3k_1}{4} & \frac{k_1}{2} \\ \frac{k_2}{2} & k_2 \end{smallmatrix}\right]$ which, for the simple selection $\alpha = (2, 4)$ leads to the following set of polynomial equations ensuring (7) (and, equivalently, (4)):

$$\left\{ \begin{array}{rcl} \frac{1}{2}k_1 k_2 & = & (\alpha_1^2 - 1)^{-1}(\alpha_2^2 - 1)^{-1} = \frac{1}{45} \\ \frac{3}{4}k_1 + k_2 & = & (\alpha_1^2 - 1)^{-1} + (\alpha_2^2 - 1)^{-1} = \frac{2}{5}. \end{array} \right. \tag{8}$$

In the general case, for a fixed value of n and fixed values in α, one can write a system of n polynomial equations in the variable k with rational coefficients, namely

$$q_i(k) = 0, \quad i = 1, \ldots, n. \tag{9}$$

Formulation (7), (9) will be used in Section 4 due to the advantageous property that all entries of each solution to this polynomial system are in the interval $(0, 1)$ as established in the next lemma.

[1] A typical selection of α is $\alpha_i = 2i$, so that the circuit resonates at the lowest possible frequency.

Lemma 2 *Given any $n \geq 1$ and any set of distinct positive even integers $\alpha = (\alpha_1, \ldots, \alpha_n)$, each solution $k = (k_1, \ldots, k_n)$ to the inverse eigenvalue problem (7) is such that $0 < k_i < 1$ for all $i = 1, \ldots, n$.*

Proof. The fact that $k_i > 0$ for all $i = 1, \ldots, n$ follows from Lemma 1 and $K = \mathrm{diag}(k_1, \ldots, k_n) = F^{-1} > 0$.

Denote now by d_i, $i = 1, \ldots, n$ the diagonal entries of B^{-1} and let us show next that $d_i \geq \frac{1}{2}$ for all $n \geq 1$, for all $i = 1, \ldots, n$. To see this, for each $i \in \{1, \ldots, n\}$, denote by e_i the i-th unit vector of the canonical basis of the Euclidean space and consider the coordinate change matrix $T = \left[\, e_i \; e_2 \; \cdots \; e_{i-1} \; e_1 \; e_{i+1} \; \cdots \; e_n \,\right]$, so that $T_i = T_i^T = T_i^{-1}$ and so that $T_i B T_i$ exchanges the 1-st and the i-th rows and columns of B. Then it is readily seen that $T_i B T_i$ is positive definite (by positive definiteness of B, as established in the proof of Lemma 3 in Section 5.2) and that the $(1,1)$ element of $T_i B^{-1} T_i = (T_i B T_i)^{-1}$ corresponds to d_i. Partition the matrix as $T_i B T_i = \begin{bmatrix} b_i & b_{i,12}^T \\ b_{i,12} & B_{i,22} \end{bmatrix}$, where b_i is the i-the diagonal element of B satisfying by construction $b_i \leq 2$. Since $B_{i,22} > 0$, the following holds by applying the matrix inversion formula to the (1,1) element of $T_i B^{-1} T_i = (T_i B T_i)^{-1}$:

$$d_i = \left(b_i - b_{i,12}^T \; B_{i,22}^{-1} \; b_{i,12}\right)^{-1} > b_i^{-1} \geq 2^{-1}. \tag{10}$$

As a next step, considering that α_i, $i = 1, \ldots, n$ are distinct positive even integers, we have that

$$\begin{aligned} \sum_{j=1}^{n} \frac{1}{\alpha_j^2 - 1} &\leq \sum_{j=1}^{n} \frac{1}{(2j)^2 - 1} = \frac{1}{2} \sum_{j=1}^{n} \frac{1}{2j-1} + \frac{1}{2j+1} \\ &= \frac{1}{2} \left[\left(1 - \frac{1}{3}\right) + \left(\frac{1}{3} - \frac{1}{5}\right) + \cdots + \left(\frac{1}{2n-1} - \frac{1}{2n+1}\right) \right] \\ &= \frac{1}{2} \left(1 - \frac{1}{2n+1}\right) \leq \frac{1}{2}. \end{aligned} \tag{11}$$

Finally, keeping in mind that the trace of KB^{-1} is the sum of its eigenvalues and considering equality (7) we can combine (10) and (11) to get

$$\frac{1}{2} \sum_{j=1}^{n} k_j < \sum_{j=1}^{n} d_j k_j = \mathrm{Tr}(KB^{-1}) = \sum_{j=1}^{n} \frac{1}{\alpha_j^2 - 1} \leq \frac{1}{2},$$

which, bearing in mind that $k_j > 0$, for all $j \in \{1, \ldots, n\}$, implies, for each $i \in \{1, \ldots, n\}$, $k_i \leq \sum_{j=1}^{n} k_j < 1$ as to be proven. □

Remark 3 (Sensitivity analysis) Sensitivity of the solution obtained by numerical techniques (or also by symbolic techniques, by truncating rational numbers to floating point numbers) can be assessed a posteriori. Indeed, the eigenvectors of a matrix encode the sensitivity of the eigenvalues to (unstructured) uncertainty affecting the entries of the matrix itself. In particular, sensitivity can be and will be assessed numerically in Section 3.2 using two main methods: a first one providing only local information by using the condition number of simple eigenvalues given in [17, §7.2.2] and a second one providing an idea

about the effect of large perturbations by graphically displaying the pseudo-spectrum of the matrix (namely the sublevel sets of the perturbed eigenvalues under norm bounded unstructured perturbations) according to [32]. As shown in Section 3.2, these tools provide useful insight about the features of different solutions leading to interesting interpretations of some of the observations in [6]. ◦

3 Symbolic solution

In this section we use techniques from real algebraic geometry to solve symbolically the inverse eigenvalue problem (2). We focus on system (6) (issued from (4)) whose polynomials p_i conveniently inherit some sparsity of the tridiagonal matrix B, in the sense that many monomials of the f_i variables are zero. In contrast, the polynomials q_i in system (9) (issued from (7)) are less sparse since matrix B^{-1} is dense.

Solving problem (6) amounts to finding a real n-dimensional solution $f = (f_1, \ldots, f_n)$ to a system of n given scalar-valued multivariate polynomial equations with rational coefficients. Throughout the paper we make the next standing assumptions on such a system of equations.

Assumption 1 *There exists a finite number of complex solutions to the system of polynomial equations (6).*

Note that Assumption 1 readily implies that there is a finite number of real solutions to the system of polynomial equations (6).

Assumption 2 *There exists at least one real solution to the system of polynomial equations (6).*

In the conclusions section we state open problems in connection with these assumptions.

3.1 Real algebraic geometry

For an elementary tutorial account of real algebraic geometry, please refer to [11]. In this paragraph we survey only a few essential ideas, with a focus on explicit algorithms.

Finding a solution to polynomial system (6) amounts to finding a point in the set

$$\mathscr{V} := \{f \in \mathbb{C}^n \ : \ p_1(f) = 0, \ldots, p_n(f) = 0\}.$$

Set $\mathscr{V}$ is a subset of $\mathbb{C}^n$ called a (complex) algebraic variety because it is the vanishing locus of a finite number of polynomials. To the geometric object $\mathscr{V}$ corresponds an algebraic object:

$$\mathscr{I} := \{a_1(f)p_1(f) + \cdots + a_n(f)p_n(f) \ : \ a_1, \ldots, a_n \in \mathbb{Q}[f]\}$$

which is a subset of $\mathbb{Q}[f]$ called an algebraic ideal. Elements in $\mathscr{I}$ are obtained by taking linear combinations (with polynomial coefficients) of polynomials p_i. We say that ideal

$\mathscr{I}$ is generated by $p_1, \ldots, p_n$, and we say that $p_1, \ldots, p_n$ is a presentation of $\mathscr{I}$. Although $\mathscr{I}$ has an infinite number of elements, it follows from a fundamental theorem of Hilbert [11, Theorem 4, §2.5] that it has always a finite presentation, and this allows $\mathscr{I}$ to be handled by a computer. Note that every polynomial in $\mathscr{I}$ vanishes at points $f \in \mathscr{V}$, and we say that $\mathscr{V}$ is the variety associated to the ideal $\mathscr{I}$.

A key idea of algebraic geometry consists in obtaining useful information on $\mathscr{V}$ from a suitable presentation of $\mathscr{I}$. By taking finitely many linear combinations of polynomials p_i, we will generate another equivalent system of polynomials which generates the same ideal $\mathscr{I}$ but with another presentation, and which is associated with the same variety $\mathscr{V}$. In particular, when $\mathscr{V}$ is a discrete set, i.e. when Assumption 1 is satisfied, this presentation should allow to compute the solutions easily. A useful presentation is a Gröbner basis [11, Section 2]. To obtain such a basis, we can devise an algorithm using only linear algebra and performing a series of multivariate polynomial divisions. These divisions can be carried out provided one defines a suitable ordering on the set of monomials of variables $f_1, \ldots, f_n$. For our purpose of computing the solutions, a useful ordering is the graded reverse lexicographic (grevlex) order, see [11, Definition 6 of Section 2.2]. Once a Gröbner basis is available, we can compute a rational univariate representation (RUR)

$$r(f_\circ) = 0,\ f_1 = \frac{r_1(f_\circ)}{r_0(f_\circ)},\ \ldots\ , f_n = \frac{r_n(f_\circ)}{r_0(f_\circ)}, \tag{12}$$

where r is a suitable univariate polynomial in a variable $f_\circ$, and $r_0, \ldots, r_n$ are univariate polynomials of degree less than the degree of r. Variable $f_\circ$ is called the separating variable, and it is a linear combination of the original variables $f_1, \ldots, f_n$.

Proposition 1 *For system (6), a Gröbner basis always exists. Moreover, all but a finite number of linear combinations of the variables f_i, $i = 1, \ldots, n$ are separating variables. Finally, once the separating variable is chosen, the RUR exists and is unique.*

Proof. The existence of a Gröbner basis follows from [11, Corollary 6, §2.5]. The rest of the proposition can be proven using [16], [27, Theorem 3.1] or [2, Proposition 12.16]. See also [31, Proposition 2.3] and the discussion just after, which explains the connection between RUR and Gröbner basis. □

Once a RUR is available, enumerating all the real solutions amounts to computing all the real roots of the univariate polynomial r in (12), and evaluating the rational functions r_i/r_0 in (12) at those points. By an appropriate use of Descartes' rule of signs and Sturm sequences, see e.g. [2, Section 2.2], an algorithm can be designed that isolates all real roots of the univariate polynomial in rational intervals of arbitrarily small width.

3.2 Numerical results and sensitivity analysis

The simplest possible selection of parameters α_i in the assignment problem (2) is to select them as the smallest possible set of distinct even and positive integers, namely $\alpha_i = 2i$ for all $i \in \{1, \ldots, n\}$. This selection gives rise to the smallest possible coefficient list in (6) and leads to a set of solutions to Problem 1 having the smallest possible maximal

frequency of the natural resonant modes of the circuit. This was also the preferred solution addressed in [35, 6]. In particular, for this specific selection of the resonant frequencies, a set of 10 solutions for the case $n = 6$ has been given in [6, Table II]. The advantage of the formal approach of this section is to allow to find the complete set of solutions, amounting to 12 (2 solutions were missed in [6, Table II] which used bounded random sampling followed by numerical optimization). Another advantage of our results is that the sets of solutions reported here were computed in a few minutes using the Maple code reported in Appendix 6. Table 1 reports the numerical values computed by the analytic algorithm proposed in this section. Note that the displayed values correspond to $n^2 c_i/c = n^2 f_i^{-1}$. We choose to represent these values to allow for an easier comparison with the results in [6, Table II] and because they are better numerically conditioned. Note that solutions number 1 and 2 for the case $n = 6$ were not reported in [6, Table II].

According to the observations reported in Remark 3 we can characterize the sensitivity of each solution obtained from the proposed symbolic solution method by looking at the condition number of each eigenvalue of matrix BF in (2). This method can be applied because all eigenvalues of BF are distinct (therefore simple) by assumption. In particular, for each eigenvalue of BF its condition number corresponds to $|w^T v|^{-1}$, where w and v have unit norm and are respectively the left and right eigenvectors associated with that eigenvalue. The results of the sensitivity analysis is represented by the maximum condition number among all eigenvalues of matrix BF and is shown in the last column of Table 1 for each one of the computed solutions.

Inspecting the different sensitivities it appears that the last solution for each one of the analyzed cases corresponds to the least sensitive one, namely the one that is expected to be more robust. Interestingly, this solution corresponds to the solution qualitatively characterized in [6] as the "regular" solution. Indeed, when looking at the time responses of the Marx generator network designed with these parameters, one experiences little dependence on higher order harmonics and some suitable monotone evolution of certain voltages in the circuit (see [6, Fig. 10] for an example of this). Another peculiar feature of the "regular" solutions corresponding to the last solution for each n in Table 1 is that the interpolated values of $n^2 c_i/c$ form a convex function of i, namely (since n^2/c is constant) one has $c_j \leq \frac{c_{j+1}+c_{j-1}}{2}$ for all $j = 2, \ldots, n-1$ (see also the red curve in [6, Fig. 8] corresponding to the last solution for $n = 6$ in Table 1). Moreover, at least up to $n = 6$, numerical evidence reveals that there only exists one such solution. Due to its desirable features both in terms of numerical robustness and of desirable time evolution of the arising circuit (as reported in [6]), we will be imposing this constraint on the numerical optimization described in the next section, to be able to isolate that specific solution for the case $n > 6$ (or all of such specific solutions, if more than one of them exist).

A final comment should be made about the use of the pseudospectra of matrix BF as a graphical tool to assess the sensitivity of each solution of Table 1 to larger perturbations. According to the results in [32] and the corresponding Matlab tool Pseudospectra GUI available in the EigTool package [32], given $\epsilon > 0$, the associated pseudospectrum of a matrix A_0 corresponds to the following region in the complex plane:

$$\{s \in \mathbb{C}\colon\ \exists \Delta \in \mathbb{C}^{n\times n}, \det(sI_n - A - \Delta) = 0,\ \text{and}\ \|\Delta\| \leq \epsilon\}$$

(see Figure 2 for some examples). Surprisingly, the graphical aspect of the pseudospectra

	$n^2\frac{c_1}{c}$	$n^2\frac{c_2}{c}$	$n^2\frac{c_3}{c}$	$n^2\frac{c_4}{c}$	$n^2\frac{c_5}{c}$	$n^2\frac{c_6}{c}$	cond
$n=1$							
1	1.5						1
$n=2$							
1	1.50213	0.47340					1.1102
2	0.63120	1.12660					1.0266
$n=3$							
1	1.49303	1.49229	0.41548				1.1557
2	0.84408	0.77662	1.41217				1.0387
$n=4$							
1	1.71070	1.29555	1.54667	0.38529			1.1849
2	1.62637	0.62519	1.73498	0.74862			1.0917
3	1.06181	2.10211	0.66491	0.89099			1.121
4	1.13210	0.78731	0.92450	1.60306			1.0440
$n=5$							
1	2.04567	1.23900	1.35694	1.57111	0.36796		1.2018
2	2.14782	0.63778	1.24610	1.70028	0.68506		1.1092
3	0.99720	1.69936	1.57266	0.64267	1.16088		1.0558
4	1.47480	0.86342	0.84481	1.07344	1.72179		1.0448
$n=6$							
1	2.49095	1.25588	1.20240	1.49359	1.53290	0.35987	1.2065
2	1.92537	1.79971	1.80083	0.90696	1.45858	0.37545	1.1954
3	1.67555	1.98118	2.05786	0.66667	1.30433	0.52174	1.112
4	2.65073	1.01602	0.68610	1.82261	1.42150	0.64738	1.1506
5	1.34706	2.18478	0.92044	1.84208	0.65432	0.94921	1.0971
6	1.95229	0.93587	1.53272	0.63062	1.76898	0.99206	1.0844
7	2.46541	0.73028	0.99423	0.93809	1.85839	0.99314	1.1223
8	1.79820	0.94167	1.74742	0.62528	1.59040	1.05327	1.0884
9	1.43355	1.89698	0.60976	1.73302	1.02388	1.05334	1.1009
10	1.50458	1.00778	2.04896	1.05339	0.68756	1.37732	1.0686
11	1.38734	1.13092	1.48392	1.32482	0.63764	1.57578	1.0617
12	1.87892	0.96056	0.85587	0.91518	1.23619	1.77345	1.0592

Table 1: The solutions to the Marx design problem computed using Gröbner basis methods and their conditioning.

appear indistinguishable among all solutions for fixed n. Nevertheless, interesting results are obtained when applying this analysis to the state transition matrix A_0 associated to the state-space model of the circuit (for fixed values of ℓ and c) whose expression is given in (17), in Section 5.1. An example of the type of pseudospectra obtained for the case $n = 5$ is represented in Figure 2 corresponding to the case $c = \ell = 1$. The figure shows that once again the "regular" solution is associated with the least sensitive scenario. Visually, this corresponds to the tightest pseudospectra (see the rightmost case in Figure 2) which can be best appreciated by inspecting the largest level set of the figure, corresponding to

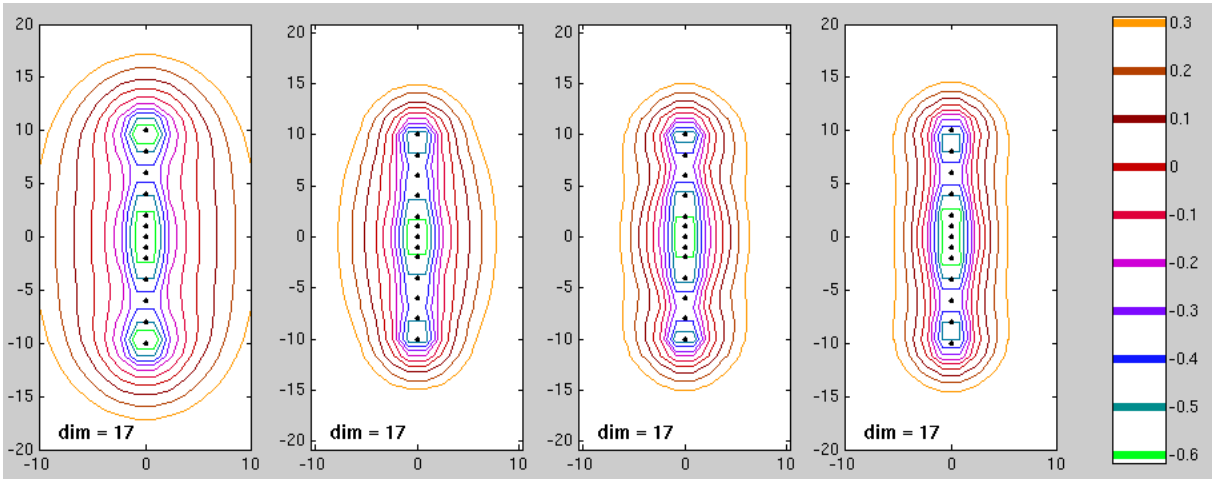

Figure 2: The pseudospectra of the state transition matrix A_0 for the four solutions corresponding to $n = 5$.

the selection $\epsilon = 10^{0.3}$ according to the legend to the right of the figure. The other values of n lead to similar results.

4 Numerical solution

In this section we use convex optimization techniques to find numerically the real solutions of our polynomial system of equation. As compared to the previous section, we focus here on the alternative formulation (9) because for this formulation, according to Lemma 2, all the real solutions satisfy $|k_i| \leq 1$, $i = 1, 2, \ldots, n$. As explained e.g. in [20], for numerical reasons it is very important that the problem unknowns are scaled down to the unit interval.

4.1 Problem formulation

A numerical approach solution to the inverse eigenvalue problem presented in Section 2.3 consists in formulating it first as a nonconvex polynomial optimization problem:

$$\begin{array}{rcll} q^* & = & \min_k & q_0(k) \\ & & \text{s.t.} & k \in \mathscr{K} \end{array} \tag{13}$$

where the objective function $q_0 \in \mathbb{Q}[k]$ is a given polynomial of the vector of indeterminates $k \in \mathbb{R}^n$, and, based on (9) and on the discussion about "regular solutions" in Section 3.2, the feasibility set

$$\begin{aligned} \mathscr{K} = \{k \in \mathbb{R}^n \ : \ & q_i(k) = 0, \ \ i = 1, \ldots, n, \\ & g_j(k) := k_j - 2k_{j+1} + k_{j+2} \geq 0, \ \ j = 1, \ldots, n-2\} \end{aligned}$$

is the real algebraic variety corresponding to the zero locus of the ideal $\mathscr{I}$ studied in Section 3 intersected with the polyhedron modeling the convexity constraints introduced in Section 3.2.

A typical objective function in problem (13) can be the positive definite convex quadratic form

$$q_0(k) = \sum_{i,j=1}^{n} (k_i - k_j)^2 = k^T \begin{bmatrix} 2 & -1 & 0 & \cdots & 0 \\ -1 & \ddots & \ddots & \ddots & \vdots \\ 0 & \ddots & \ddots & \ddots & 0 \\ \vdots & \ddots & \ddots & 2 & -1 \\ 0 & \cdots & 0 & -1 & 2 \end{bmatrix} k$$

so that capacitors $c_i = k_i/c$ are as identical as possible, but we can also consider other relevant objective functions, not necessarily quadratic, definite in sign or convex.

Optimization problem (13) is finite-dimensional, algebraic, but nonconvex since the feasibility set $\mathscr{K}$ is disconnected, as a union of isolated points (because of Assumption 1). Local optimization techniques based on nonlinear programming are likely to face troubles with such sets. Function q_0 is continuous and we optimize it over $\mathscr{K}$ which is compact, since by Assumptions 1 and 2 there is at least one real solution and at most a finite number of isolated real solutions. It follows that optimization problem (13) has at least one solution. Since q_0 is not necessarily convex and $\mathscr{K}$ is disconnected, we do not expect optimization problem (13) to have a unique global minimizer. However, we expect the number of global minimizers to be significant smaller than the cardinality of set $\mathscr{K}$.

4.2 Optimization method using Gloptipoly

Our optimization method is based on an idea first described in [22] which consists in reformulating a nonconvex global optimization problem with polynomial data (i.e. minimization of a polynomial objective function subject to polynomial inequalities and/or equations) as an equivalent convex linear programming (LP) problem over probability measures. Instead of optimizing over a vector in a finite-dimensional Euclidean space, we optimize over a probability measure in an infinite-dimensional Banach space. The measure is supported on the feasibility set of the optimization problem, which is algebraic in our case, and we require in addition that the set is bounded (which is true in our case, by assumption). More concretely, a probability measure is understood as a linear functional acting on the space of continuous functions, and we manipulate a measure through its moments, which are images of monomials (which are dense w.r.t. the supremum norm in the space of continuous functions with compact support). Using results on functional analysis and real algebraic geometry, and under some mild assumption on the compact support, a sequence of real numbers are moments of a probability measure if they belong to an appropriate affine section of the cone of positive semidefinite linear operators, an infinite-dimensional convex set. We then construct a hierarchy of finite-dimensional truncations of this convex set, namely affine sections of the cone of positive semidefinite matrices of fixed size. As a result, solving an LP in the set of probability measures with compact semi-algebraic support boils down to solving a hierarchy of semidefinite programming (SDP) problems, also called linear matrix inequalities (LMIs).

When there is a finite number of global optimizers, the approach is guaranteed to converge in a finite number of steps, and the global optimizer(s) can be extracted with the help of numerical linear algebra, see [20]. We have then a numerical certificate of global optimality of the solution(s). This approach has been successfully applied to solve globally various polynomial optimization problems, see [25] and [23] for general overviews of results and applications. For applications in systems control, the reader is referred to the survey [19]. For finding real solutions of systems of polynomial equations and real radical ideals, the approach has been comprehensively studied in [24].

More explicitly, we now describe our approach to the numerical solution of problem (13). We consider a compact set $\mathscr{K} \subset \mathbb{R}^n$ and we denote by $\mathscr{M}(\mathscr{K})$ the Banach space of Borel measures supported on $\mathscr{K}$. These are nonnegative functions from the Borel sigma-algebra of subsets of $\mathscr{K}$ to the real line $\mathbb{R}$. Given a measure $\mu \in \mathscr{M}(\mathscr{K})$ we define its moment of order $\alpha \in \mathbb{N}^n$ as the real number [2]

$$y_\alpha = \int_{\mathscr{K}} x^\alpha \mu(dx) \in \mathbb{R} \tag{14}$$

where we use the multi-index notation for monomials, i.e. $x^\alpha = \prod_{i=1}^n x_i^{\alpha_i}$. We define the infinite-dimensional vector $y = \{y_\alpha\}_{\alpha \in \mathbb{N}^n}$ as the sequence of moments of μ. Note that $y_0 = \int \mu = \mu(\mathscr{K}) = 1$ whenever $\mu \in \mathscr{M}(\mathscr{K})$ is a probability measure. Moreover, if for each $k \in \mathscr{K}$, $|k_i| \leq 1$ for all i (this is what we establish in Lemma 2), then $|y_\alpha| \leq 1$ for all $\alpha \in \mathbb{N}^n$. Conversely, for larger sets $\mathscr{K}$, the variable y_α may grow very large and this is not convenient for numerical reasons. This aspect has been pointed out in [20] and motivates Lemma 2.

Given a sequence y, we define the Riesz linear functional $\ell_y : \mathbb{R}[x] \to \mathbb{R}$ which acts on polynomials $\pi(x) = \sum_\alpha \pi_\alpha x^\alpha$ as follows: $\ell_y(\pi(x)) = \sum_\alpha \pi_\alpha y_\alpha$. If sequence y has a representing measure μ, integration of polynomial $\pi(x)$ w.r.t. μ is obtained by applying the Riesz functional ℓ_y on $\pi(x)$, since $\ell_y(\pi(x)) = \int \pi(x)\mu(dx) = \int \sum_\alpha \pi_\alpha x^\alpha \mu(dx) = \sum_\alpha \pi_\alpha \int x^\alpha \mu(dx) = \sum_\alpha \pi_\alpha y_\alpha$.

If we apply the Riesz functional on the square of a polynomial $\pi(x)$ of degree d, then we obtain a form which is quadratic in the coefficient vector $\pi = \{\pi_\alpha\}_{|\alpha| \leq d}$ and which we denote

$$\ell_y(\pi^2(x)) = \pi^T M_d(y) \pi$$

where $M_d(y)$ is a symmetric matrix which is linear in y, called the moment matrix of order d. Rows and columns in this matrix are indexed by vectors $\alpha \in \mathbb{N}^n$ and $\beta \in \mathbb{N}^n$, and inspection reveals that indeed the entry (α, β) in matrix $M_d(y)$ is the moment $y_{\alpha+\beta}$. Given a polynomial $\chi(x)$ we let

$$\ell_y(\pi^2(x)\chi(x)) = \pi^T M_d(\chi, y) \pi$$

where $M_d(\chi, y)$ is a symmetric matrix which is linear in y and linear in coefficients of $\chi(x)$, called the localizing matrix of order d w.r.t. $\chi(x)$. The localizing matrix is a linear combination of moment matrices, in the sense that entry (α, β) in $M_d(\chi, y)$ is equal to $\sum_\gamma \chi_\gamma y_{\alpha+\beta+\gamma}$.

[2] The notation α_i is used in (14) and the remaining derivations in this section, for consistency with the notation used in [22] and references therein. However, they should not be confused with the scalars α_i used in Theorem 1.

4.3 Application to the eigenvalue assignment problem

Based on the optimization method presented in the previous section, we now formulate the polynomial optimization problem (13) as a hierarchy of finite-dimensional LMI problems with the help of the Matlab interface GloptiPoly 3 [21]. Then, we use public-domain implementations of primal-dual interior point algorithms to solve the LMI problems. These algorithms rely on a suitable logarithmic barrier function for the SDP cone, and they proceed by iteratively reducing the duality gap between the primal problem and its dual, which is also an LMI problem. Each iteration consists in solving a Newton linear system of equations, involving the gradient and the Hessian of a Lagrangian built from the barrier function. Most of the computational burden comes from the construction and the storage of the Hessian matrix, and problem sparsity can be largely exploited at this stage. For more information on SDP and related optimization methods, see e.g. [4]. For our numerical examples we have been using the SDP solver SeDuMi 1.3 [30].

More specifically, let $d_i = \lceil \frac{\deg q_i}{2} \rceil$, $i = 0, 1, \ldots, n$, and consider the optimization problem

$$\begin{array}{rcll} q_d^* & = & \inf_y & \ell_y(q_0) \\ & & \text{s.t.} & y_0 = 1 \\ & & & M_d(y) \succeq 0 \\ & & & M_{d-d_i}(q_i, y) = 0, \quad i = 1, \ldots, n \\ & & & M_{d-1}(g_j, y) \succeq 0, \quad j = 1, \ldots, n-2 \end{array} \tag{15}$$

for $d \geq \max\{d_i\}_{i=0,1,\ldots,n}$, where $\succeq 0$ stands for positive semidefinite.

In the above problem, the unknown is the truncated sequence y of moments of degree up to $2d$, and the constraints are convex linear matrix inequalities (LMI) in y. Problem (15) is called the LMI relaxation of order d of problem (13). It can be proved that the infimum in LMI problem (15) is attained, as stated in the next proposition which is proven in [23, Theorem 6.1].

Proposition 2 *The optimal values of (15) satisfy $q_d^* \leq q_{d+1}^*$. Moreover, under Assumptions 1 and 2 there exists a finite $d^* \in \mathbb{N}$ such that $q_d^* = q^*$ for all $d \geq d^*$, where q^* is the optimal value of (13).*

Roughly speaking, Proposition 2 establishes that the solutions to the sequence of relaxations converge at a finite (although unknown) value of $d = d^*$, so that solving LMI (15) is equivalent to solving problem (13). We should remark that while LMI solutions are not very accurate, they can be obtained cheaply (at least for these examples) since we do not need to enumerate all real solutions, only the optimal one(s). Moreover, if a computed solution is not deemed accurate enough, it can be refined locally afterwards by Newton's method if required.

Remark 4 Proposition 2 states that solving nonconvex polynomial optimization (13) is equivalent to solving convex LMI problem (15) for a sufficiently large relaxation order d^* if the feasibility set has zero dimension and is nonempty . Unfortunately, it is not possible to give a priori useful (lower or upper) bounds on d^*, and the strategy followed in [20] is

to detect global optimality of an LMI relaxation by inspecting the rank of the moment matrix and then extract the globally optimal solutions by linear algebra, see also [24] and [23, Algorithm 6.1]. For all the Marx generator design problems that we considered, we observed that the global optimum is certified at the smallest possible LMI relaxation, i.e., in Proposition 2, $d^* = \max\limits_{i=0,1,\ldots,n} \left\lceil \frac{\deg q_i}{2} \right\rceil = \left\lceil \frac{n}{2} \right\rceil$. ∘

4.4 Numerical results and sensitivity analysis

We applied this numerical approach on our examples, with different objective functions, and the overall conclusion is that the cases $n = 2, 3, 4, 5$ are solved very easily (in a few seconds) but the solution (obtained with SeDuMi) is not very accurate. The case $n = 6$ is solved in a few minutes, and the case $n = 7$ is significantly harder: it takes a few hours to be solved and it provides the following "regular" solution (in the sense introduced in Section 3.2):

$n^2\frac{c_1}{c}$	$n^2\frac{c_2}{c}$	$n^2\frac{c_3}{c}$	$n^2\frac{c_4}{c}$	$n^2\frac{c_5}{c}$	$n^2\frac{c_6}{c}$	$n^2\frac{c_7}{c}$
2.07061	1.05669	1.04940	1.05715	1.06861	1.08449	1.85298

For this solution, we can compute the sensitivity level using the same algorithm used in the last column of Table 1 and we obtain 1.0502. Finally, solving the case $n = 8$ takes approximately 15 hours and leads to the following set of parameters. The sensitivity of this solution corresponds to 1.0617. Figure 3 shows a time history of the corresponding response with $c = \ell = 1$, with the notation introduced later in Figure 4. The simulation shows that all the energy initially stored in the storage capacitors is transferred to the load capacitor (note that the black curve in the lower plot represents v_L/n). Note also that the eight storage and parasitic voltages are characterized by an ordering which remains constant along the whole trajectory, which is a peculiar feature of the so-called "regular" solution (note that a similar behavior is obtained for the regular solution associated with $n = 6$, as reported in [6, Fig. 10]).

$n^2\frac{c_1}{c}$	$n^2\frac{c_2}{c}$	$n^2\frac{c_3}{c}$	$n^2\frac{c_4}{c}$	$n^2\frac{c_5}{c}$	$n^2\frac{c_6}{c}$	$n^2\frac{c_7}{c}$	$n^2\frac{c_8}{c}$
2.39407	1.17326	1.12475	1.11221	1.10440	1.09960	1.09985	1.87282

5 Circuit description and proofs

We carry out the proof of Theorem 1 by first providing a mathematical description of the circuit (Section 5.1), then proving a useful resonance result (Section 5.2) and then proving the theorem (Section 5.3).

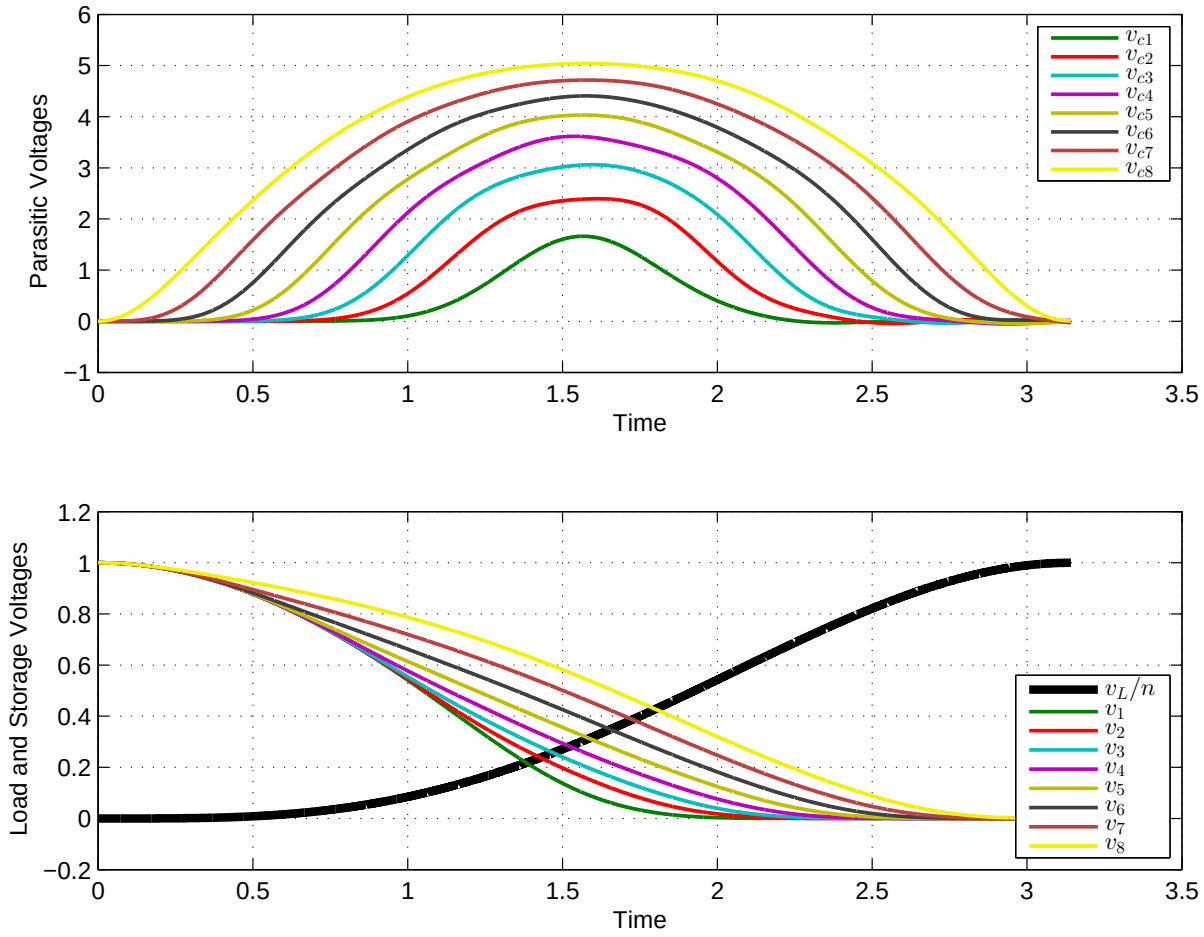

Figure 3: Time histories of the parasitic capacitor voltages (upper plot) and of the load and storage capacitors voltages (bold and solid curves in lower plot) for the regular solution to the case $n = 8$ found via numerical optimization.

5.1 Circuit description

Following an approach similar to the one adopted in [1], it is possible to derive a state-space representation of the Marx generator of Figure 1 using $3n + 2$ state variables comprising $2n+1$ voltages across the $2n+1$ circuit capacitors, and $n+1$ currents flowing in the $n+1$ inductors.

In particular, using the sign convention and the component values depicted in Figure 4 (see also Figure 1), we can define the state variable as

$$x = [v_{c1}, \cdots, v_{cn}, v_1, \cdots, v_n, v_{n+1}, i_1, \cdots, i_n, i_L]^T, \tag{16}$$

(note that i_L has opposite direction to the other currents to simplify the derivations in the proof of Theorem 1) and the linear dynamics of the circuit correspond to the equations

$$c\dot{v}_k = i_k, \ k = 1, \ldots, n, \quad c\dot{v}_{n+1} = i_L,$$
$$\ell\dot{i}_1 = v_{c1} - v_1, \quad n\ell\dot{i}_L = v_{cn} - nv_{n+1},$$

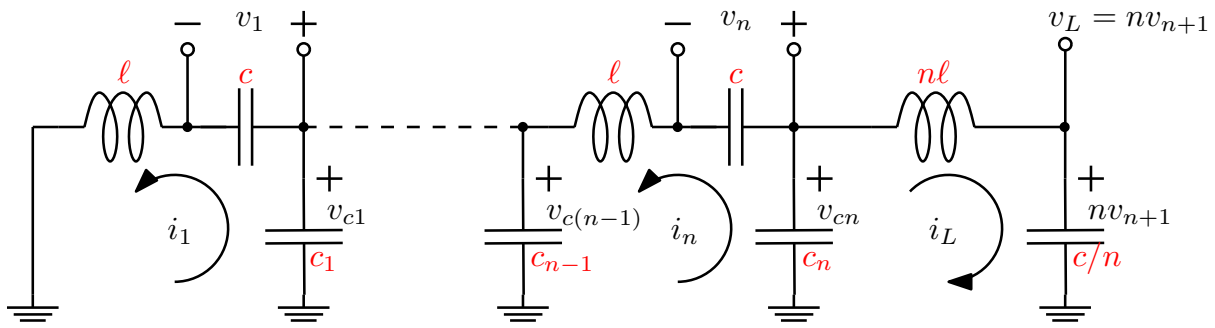

Figure 4: Sign conventions in the models of the Marx generator circuit.

$$\ell \dot{i}_k = v_{ck} - v_{c(k-1)} - v_k,\ k = 2, \dots, n,$$
$$c_k \dot{v}_{ck} = i_{k+1} - i_k,\ k = 1, \dots, n-1, \quad c_n \dot{v}_{cn} = -i_L - i_n,$$

which can be written in compact form using the following linear state-space model $\dot{x} = A_0 x$ where

$$A_0 := \left[\begin{array}{cc|c} & & -\frac{1}{c} F \Sigma J_{-1} \\ & 0_{(2n+1)\times(2n+1)} & \frac{1}{c} I_{n+1} \\ \hline \frac{1}{\ell} J_{n+1}^{-1} J_{-1} \Sigma^T & -\frac{1}{\ell} I_{n+1} & 0_{(n+1)\times(n+1)} \end{array}\right], \tag{17}$$

where $0_{q\times q} \in \mathbb{R}^{q\times q}$ is a square matrix of zeros, I_q is the identity matrix of size q, $J_{n+1} = \mathrm{diag}(1, \dots, 1, n) \in \mathbb{R}^{(n+1)\times(n+1)}$, $J_{-1} = \mathrm{diag}(1, \dots, 1, -1) \in \mathbb{R}^{n\times n}$ are both diagonal matrices, $\Sigma = \begin{bmatrix} 1 & -1 & 0 & \cdots & 0 \\ 0 & 1 & -1 & \cdots & 0 \\ \vdots & \vdots & \ddots & \ddots & \vdots \\ 0 & \cdots & 0 & 1 & -1 \end{bmatrix} \in \mathbb{R}^{n\times(n+1)}$ and F is defined in the statement of Theorem 1.

5.2 A sufficient resonance condition

In this section we establish a preliminary result that will be useful for the proof of Theorem 1 and which is based on the description (17) of the generator dynamics.

Lemma 3 *Consider the Marx circuit in Figure 1 and the matrices B in (1) and $F = \mathrm{diag}(c/c_1, \dots, c/c_n)$. The matrix $I + BF$ has n real positive eigenvalues. Moreover, denoting by $a_1^2, \dots, a_n^2$ such n real positive eigenvalues and fixing $a_0 = 1$, matrix A_0 in (17) has n eigenvalues in $s = 0$ having n distinct eigenvectors, and $n+1$ pairs of purely imaginary conjugate eigenvalues in $s = \pm \jmath \omega_0 a_k$, $k = 0, \dots, n$.*

Proof. First, we establish that $I + BF$ has n positive eigenvalues. This follows from the coordinate change $T = \sqrt{F}$ transforming the matrix into $I + \sqrt{F} B \sqrt{F}$, which is a symmetric positive definite matrix because I is such and $B = \Sigma J_{n+1}^{-1} \Sigma^T$ is positive definite. For later use, define $\bar{B} := \sqrt{F} B \sqrt{F}$ and N, $\bar{N}$ by the relations $N^T N = (I + \bar{B}) = \bar{N}^T \Lambda^2 \bar{N}$, with $\Lambda = \mathrm{diag}(a_1, \dots, a_n)$ and $\bar{N}^{-1} = \bar{N}^T$, that is $\bar{N}$ is orthonormal (such factorizations are possible since $I + \bar{B}$ is positive definite).

In order to highlight the eigenstructure of A_0, a sequence of coordinate transformations will be used. Consider a first change of coordinates $A_1 = T_0 A_0 T_0^{-1}$ with

$$T_0 = \text{blkdiag}\left(-\sqrt{\frac{c}{\ell}F^{-1}},\ \sqrt{\frac{c}{\ell}J_{n+1}},\ \sqrt{J_{n+1}}\right), \tag{18}$$

which yields (recalling that $\omega_0 := (\sqrt{\ell c})^{-1}$)

$$A_1 := \omega_0 \left[\begin{array}{cc|c} & & M \\ & 0_{(2n+1)\times(2n+1)} & \\ & & I_{n+1} \\ \hline -M^T & -I_{n+1} & 0_{(n+1)\times(n+1)} \end{array}\right], \tag{19a}$$

$$M := \sqrt{F}\Sigma J_{-1}\sqrt{J_{n+1}^{-1}}, \tag{19b}$$

Note that since $\text{Im}(\Sigma) = \mathbb{R}^n$ and $\ker(\Sigma) = \text{Im}(1_{n+1})$, where 1_{n+1} is the vector in $\mathbb{R}^{n+1}$ having all components equal to 1, it follows that

$$\text{Im}(M) = \mathbb{R}^n,\ \ker(M) = \text{Im}(\nu),\ \nu := \sqrt{J_{n+1}}J_{-1}1_{n+1},$$

and the matrix $[\nu\ M^T] \in \mathbb{R}^{n+1}$ is invertible since by well known results $\text{Im}(M)\oplus\ker(M) = \mathbb{R}^{n+1}$.

Since A_1 in (19a) is real and skew symmetric, its eigenvalues are either zero or in imaginary conjugate pairs. To explicitly show them and the corresponding real invariant subspaces, consider matrix V given by

$$V = \left[\begin{array}{ccccc} I_n & 0 & 0 & \bar{B} & 0 \\ -M^T & \nu & 0 & M^T & 0 \\ 0 & 0 & \nu & 0 & M^T N^T \end{array}\right]. \tag{20}$$

Invertibility of V can be seen by computing VS_1S_2, with

$$S_1 = \left[\begin{array}{ccccc} I_n & 0 & 0 & 0 & 0 \\ 0 & 1 & 0 & 0 & 0 \\ 0 & 0 & 0 & 1 & 0 \\ I_n & 0 & I_n & 0 & 0 \\ 0 & 0 & 0 & 0 & (N^T)^{-1} \end{array}\right],\ S_2 = \left[\begin{array}{ccccc} (I_n+\bar{B})^{-1} & 0 & -(I_n+\bar{B})^{-1}\bar{B} & 0 & 0 \\ 0 & 1 & 0 & 0 & 0 \\ 0 & 0 & I_n & 0 & 0 \\ 0 & 0 & 0 & 1 & 0 \\ 0 & 0 & 0 & 0 & I_n \end{array}\right],$$

yielding

$$VS_1S_2 = \left[\begin{array}{ccccc} I_n+\bar{B} & 0 & \bar{B} & 0 & 0 \\ 0 & \nu & M^T & 0 & 0 \\ 0 & 0 & 0 & \nu & M^T \end{array}\right] S_2 = \left[\begin{array}{ccccc} I_n & 0 & 0 & 0 & 0 \\ 0 & \nu & M^T & 0 & 0 \\ 0 & 0 & 0 & \nu & M^T \end{array}\right].$$

It is then possible to consider the additional change of coordinates $A_2 = T_1 A_1 T_1^{-1}$ where $T_1 = V^{-1}$. The computation of A_2 is immediate by expressing A_1V as VA_2, which yields

$$A_2 := \omega_0 \left[\begin{array}{c|cc|cc} 0_{n\times n} & 0 & & 0 & \\ \hline 0 & 0 & 1 & 0 & \\ & -1 & 0 & & \\ \hline 0 & 0 & & 0_{n\times n} & N^T \\ & & & -N & 0_{n\times n} \end{array}\right]. \tag{21}$$

Due to the block diagonal structure of A_2, it is clear that it has n eigenvalues equal to 0, a pair of imaginary eigenvalues at $\pm\jmath\omega_0$, and the remaining eigenvalues equal to ω_0 times the eigenvalues of

$$\begin{aligned}\begin{bmatrix} 0_{n\times n} & N^T \\ -N & 0_{n\times n}\end{bmatrix} &= \begin{bmatrix} I_n & 0 \\ 0 & \bar{N}\end{bmatrix}\begin{bmatrix} 0_{n\times n} & \Lambda \\ -\Lambda & 0_{n\times n}\end{bmatrix}\begin{bmatrix} I_n & 0 \\ 0 & \bar{N}^{-1}\end{bmatrix} \\ &= \begin{bmatrix} I_n & 0 \\ 0 & \bar{N}\end{bmatrix}\left(\begin{bmatrix} 0 & 1 \\ -1 & 0\end{bmatrix}\otimes\Lambda\right)\begin{bmatrix} I_n & 0 \\ 0 & \bar{N}^{-1}\end{bmatrix},\end{aligned}$$

which are equal to $\pm\jmath a_i$, $i = 1,\dots,n$ since the eigenvalues of a Kronecker product of two matrices are given by all the possible products between an eigenvalue of the first matrix (in this case, $\pm\jmath$) and an eigenvalue of the second matrix (in this case, a_i, $i = 1,\dots,n$). □

5.3 Proof of Theorem 1

Consider the circuit of Figure 1 and its state space equations with the state x given in (16). In the following reasoning, we will use the coordinates $\tilde{x} = \tilde{T}x$ and $\hat{x} = T_0 x = T_1^{-1}\tilde{x}$, where $\tilde{T} = T_1 T_0$.

Considering the initial state as in the statement of Problem 1, namely $x_0 = v_\circ[0_n^T\ 1_n^T\ 0_{n+2}^T]^T$, our aim is to show that the corresponding free response will yield $x(T) = v_\circ[0_{2n}^T\ 1\ 0_{n+1}^T]^T$.

In the $\hat{x}$ coordinates, the initial state x_0 becomes $\hat{x}_0 = c_0[0_n^T\ 1_n^T\ 0_{n+2}^T]^T$ with $c_0 = v_\circ\sqrt{\frac{c}{\ell}}$. The corresponding expression of $\tilde{x}_0$ can be found by the relation $\hat{x}_0 = T_1^{-1}\tilde{x}_0$ with $T_1^{-1} = V$ given by (20); partitioning $\tilde{x}_0$ according to the block columns of V, and choosing $\delta_0 := (I_n + \bar{B})^{-1}\sqrt{F^{-1}}\delta$, $\delta := [1\ 2\ \dots\ n]^T$, it follows that $\tilde{x}_0 = \frac{c_0}{2}\begin{bmatrix} -\bar{B}\delta_0 \\ 1 \\ 0 \\ \delta_0 \\ 0\end{bmatrix}$. In fact, it is possible to verify that

$$\begin{aligned}V\tilde{x}_0 &= \begin{bmatrix} I_n & 0 & 0 & \bar{B} & 0 \\ -M^T & \nu & 0 & M^T & 0 \\ 0 & 0 & \nu & 0 & M^T N^T\end{bmatrix}\frac{c_0}{2}\begin{bmatrix} -\bar{B}\delta_0 \\ 1 \\ 0 \\ \delta_0 \\ 0\end{bmatrix} \\ &= \frac{c_0}{2}\begin{bmatrix} 0 \\ M^T\sqrt{F^{-1}}\delta + \nu \\ 0\end{bmatrix} = \begin{bmatrix} 1_n \\ 0\end{bmatrix} = \hat{x}_0,\end{aligned}$$

by using the following relation:

$$\begin{aligned}M^T\sqrt{F^{-1}}\delta + \nu &= J_{-1}\sqrt{J_{n+1}^{-1}}\left(\Sigma^T\delta + J_{n+1}1_{n+1}\right) \\ &= J_{-1}\sqrt{J_{n+1}^{-1}}\left(\begin{bmatrix} 1_n \\ -n\end{bmatrix} + \begin{bmatrix} 1_n \\ n\end{bmatrix}\right) = 2\begin{bmatrix} 1_n \\ 0\end{bmatrix}.\end{aligned}$$

Decompose now $\tilde{x}_0$ as $\tilde{x}_0 = \tilde{x}_{01} + \tilde{x}_{02} + \tilde{x}_{03}$ with

$$\tilde{x}_{01} = \frac{c_0}{2}\begin{bmatrix} -\bar{B}\delta_0 \\ 0_{2n+2}\end{bmatrix}, \tilde{x}_{02} = \frac{c_0}{2}\begin{bmatrix} 0_n \\ 1 \\ 0 \\ 0_{n+1}\end{bmatrix}, \tilde{x}_{03} = \frac{c_0}{2}\begin{bmatrix} 0_{n+2} \\ \delta_0 \\ 0\end{bmatrix},$$

and consider that, according to the structure in (21), $\tilde{x}_{01}$ only excites constant modes, $\tilde{x}_{02}$ only excites modes at frequency ω_0 (which have a phase change between $t=0$ and $t=T$ of exactly $\omega_0 T = \pi$), and $\tilde{x}_{03}$ only excites modes at frequency $\alpha_i\omega_0$, $i=1,\ldots,n$ with α_i even (which have a phase change between $t=0$ and $t=T$ of exactly $\alpha_i\omega_0 T = 2h\pi$, with $h \in \mathbb{N}$). It follows that

$$\tilde{x}(T) = \tilde{x}_{01} + \tilde{x}_{03} - \tilde{x}_{02},$$

and then

$$\begin{aligned}
\hat{x}(T) = V(\tilde{x}_{01} + \tilde{x}_{03} - \tilde{x}_{02}) &= \frac{c_0}{2}\begin{bmatrix} 0_n \\ M^T\sqrt{F^{-1}}\delta - \nu \\ 0_{n+1} \end{bmatrix}, \\
\frac{c_0}{2}(M^T\sqrt{F^{-1}}\delta - \nu) &= \frac{c_0}{2} J_{-1}\sqrt{J_{n+1}^{-1}}\left(\begin{bmatrix} 1_n \\ -n \end{bmatrix} - \begin{bmatrix} 1_n \\ n \end{bmatrix}\right) \\
&= c_0 \begin{bmatrix} 0_n \\ \sqrt{n} \end{bmatrix},
\end{aligned}$$

and finally, computing $x(T) = T_0^{-1}\hat{x}(T)$, the desired result $x(T) = v_\circ[0_{2n}^T \ 1 \ 0_{n+1}^T]^T$ is obtained, which corresponds to having $v_{n+1}(T) = v_\circ$ and all other voltages and currents at zero, which in turn implies $v_L(T) = nv_{n+1}(T) = nv_\circ$, as to be proven.

6 Conclusion and perspectives

We proved that the design of an n-stage Marx generator electrical network exhibiting a desirable energy transfer boils down to a structured pole assignment. This can be in turn formulated as a structured system of n polynomial equations in n unknowns with rational coefficients. We have then illustrated a symbolic and a numerical approach to the computation of its solutions. By extrapolating from the analyzed cases, we conjecture that there is a finite number of complex, hence real solutions to this polynomial system. We also conjecture that there is at least one real solution. This motivates our Assumptions 1 and 2. The degrees of the polynomials are equal to $1, 2, \ldots, n$ so that the Bézout bound on the number of complex solutions, as well as the mixed volume of the support polytopes of the polynomials [31, Section 3], both equal $n!$. The number of computed real solutions is however much less than this upper bound. It would be insightful to study the applicability of existing upper and lower bounds on the number of real solutions of systems of polynomial equations, see [29] for a recent survey.

We solve the polynomial system of equations first with a symbolical method, namely Gröbner bases and rational univariate representations. All real solutions are then obtained from the real roots of a univariate polynomial of degree $n!$. This univariate polynomial can be computed exactly (i.e. with rational coefficients) and its real roots are isolated in rational intervals at any given relative accuracy. Using state-of-the-art implementation of Gröbner basis algorithms, we could solve the equations up to $n = 6$ stages routinely on a standard computer. Then we solved the same system of polynomial equations with a numerical method, using Lasserre's hierarchy of convex LMI relaxations for polynomial optimization. The advantage of this approach is that it is not necessary to represent or

enumerate all $n!$ complex solutions, and a particular real solution optimal with respect to a given polynomial objective function can be found quite easily up to $n = 8$. The accuracy of the computed solutions may not be very good, but this can be refined locally afterwards using, e.g. Newton's method. Future work may involve the use of alternative solution methods such as, e.g., homotopy or continuation algorithms [33, 18, 3].

Acknowledgments

We are grateful to Mohab Safey El Din for technical input on solving polynomial system of equations. We also thank Chaouki T. Abdallah and Edl Schamiloglu for helpful discussions. Finally, we thank M. Francaviglia and A. Virzì for their preliminary work on this subject.

Appendix

In this appendix, we comment on some sample Maple and Matlab implementations of the symbolic and numerical algorithms described in Sections 3 and 4, respectively.

Symbolic algorithm

To solve the polynomial system of equations (6) we use special computing packages which can be called directly from inside a computing sheet of the Maple computation software.

The first step computes a Gröbner basis in grevlex ordering. This is achieved by means of the `fgb_gbasis` procedure of the `FGB` package, see [14, 15]. This implementation of Gröbner basis computation is considered to be one of the most efficient available. To speed up linear algebra computations, the algorithm works in an integer ring with prime characteristic, for a sufficient large prime number found iteratively. Then, for finding the real solutions, a RUR is computed from the Gröbner basis, see [27]. Finally, for isolating the real roots of the univariate polynomial, the procedure `rs_isolate_gb` in the `fgbrs` package is used. It returns small rational intervals (as small as one wants) within which the roots are guaranteed to be found. See [28] for further references on the method used.

The whole process lies in a few lines of Maple code. We first generate the polynomial system (corresponding to (6)), denoted by `p` in the following Maple sheet:

```
with(LinearAlgebra):with(PolynomialTools):
n:=4:B:=Matrix(n):
for i from 1 to n-1 do
 B(i,i):=2: B(i,i+1):=-1: B(i+1,i):=-1:
end do:
B(n,n):=(n+1)/n;
F:=Matrix(n,Vector(n,symbol=f),shape=diagonal):
d:=product(x-((2*j)^2-1),j=1..n):
```

```
p:=CoefficientList(collect(
   charpoly(B.F,x)-d,x),x);
```

We then use the `FGb` package to transform the system `p` in a new algebraic system referenced with the name `GB`:

```
with(FGb):
fv:=[seq(f[i],i=1..n)]:
GB:=fgb_gbasis(p,0,fv,[]):
```

Finally, the solutions are computed as follows:

```
with(fgbrs):
rs_isolate_gb(GB,fv);
```

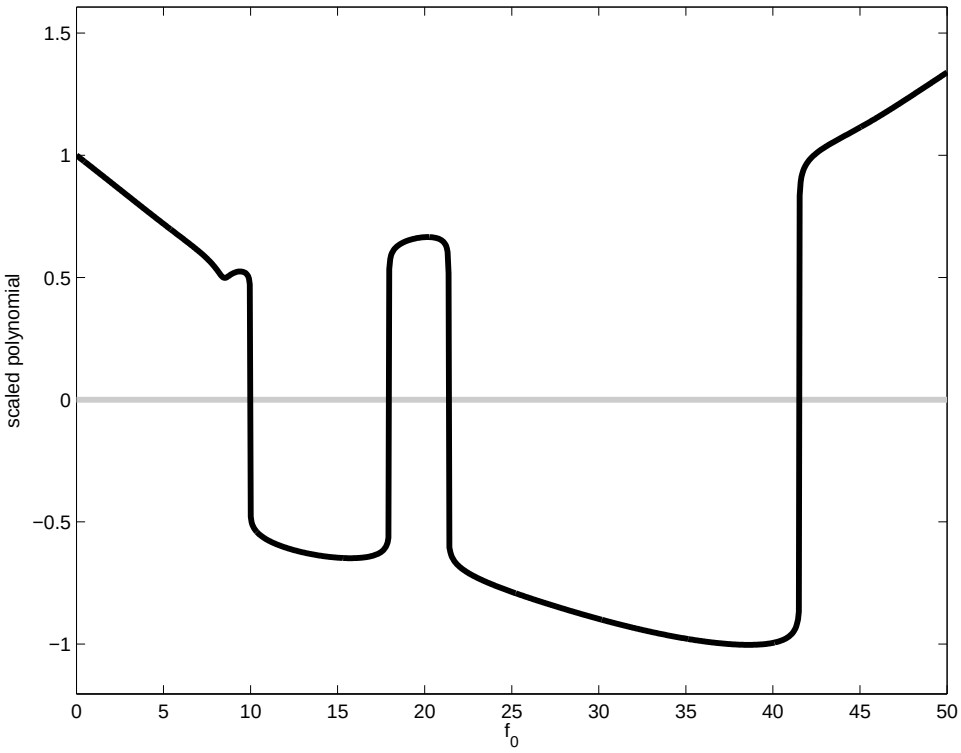

Figure 5: Case $n = 4$: rescaled graph of the univariate polynomial whose 4 real roots parametrize the 4 real solutions of the polynomial equations (6).

As an example, in the case $n = 4$ the univariate polynomial $r(f_\circ)$ that enters the RUR (12) has degree 24, and it parametrizes all the $4! = 24$ (complex) solutions. Out of 24, only 4 solutions are real. This polynomial, or rather its scaled version

$$f_\circ \mapsto \mathrm{sign}(r(f_\circ))\,|r(f_\circ)|^{\frac{1}{24}},$$

which allows to more easily visualize its zero crossings, is represented in Figure 5. It is computed as follows

```
with(Groebner):
R:=RationalUnivariateRepresentation(GB,x):
r:=R[1];
```

In practice, the computation of a Gröbner basis becomes very hard as n, the number of variables and equations, increases. For the specific system of equations (6) associated to the formulation (4) of the Marx generator design, we observe that for $2 \leq n \leq 6$ the univariate polynomial $r(f_\circ)$ of the RUR has degree $n!$. Moreover, the size of the (integer) coefficients of this polynomial are very large. If one compares the degree of the polynomial, 720 in the case $n = 6$, and the number of real roots, 12 in this case, it is clear that the computation complexity is due to the very large number of complex roots, which are of no interest for our engineering problem.

Numerical algorithm for $n = 3$

First we generate the polynomials $q_i(k)$, $i = 1, \ldots, n$ corresponding to (9) and defining the feasibility set $\mathscr{K}$ in problem (13). We use the following Maple code, where we select $\alpha_i = 2i$, $i = 1, \ldots, n$ just like in Section 3.2:

```
with(LinearAlgebra):with(PolynomialTools):
n:=3:B:=Matrix(n):for i from 1 to n-1 do
 B(i,i):=2: B(i,i+1):=-1: B(i+1,i):=-1:
end do: B(n,n):=(n+1)/n;
K:=Matrix(n,Vector(n,symbol=k),
          shape=diagonal):
p:=product(x-1/((2*j)^2-1),j=1..n):
q:=CoefficientList(collect(
    charpoly(MatrixInverse(B).F,x)-p,x),x);
```

For $n = 3$ this code generates the following polynomials

$$\begin{aligned} q_1(k) &= -\tfrac{3}{7} + \tfrac{5}{6}k_1 + \tfrac{4}{3}k_2 + \tfrac{3}{2}k_3 \\ q_2(k) &= -\tfrac{53}{1575} + \tfrac{2}{3}k_1k_2 + k_1k_3 + k_2k_3 \\ q_3(k) &= -\tfrac{1}{1575} + \tfrac{1}{2}k_1k_2k_3. \end{aligned}$$

These polynomials are then converted into Matlab format, and we use the following GloptiPoly code for inputing problem (13) and solving the smallest possible LMI relaxation, i.e. $d = \lceil \frac{3}{2} \rceil = 2$ in problem (15) (note also the inequality constraints in `P` corresponding to the convexity requirement for the "regular" solution):

```
mpol k 3
K = [-3/7+5/6*k(1)+4/3*k(2)+3/2*k(3)
     -53/1575+2/3*k(1)*k(2)+k(1)*k(3)+k(2)*k(3)
     -1/1575+1/2*k(1)*k(2)*k(3)];
obj = 0;
for i = 1:length(k)
```

```
 for j = 1:length(k)
  obj = obj+(k(i)-k(j))^2;
 end
end
P = msdp(min(obj),K==0,k(1)-2*k(2)+k(3)>=0);
[stat,obj] = msol(P);
double(k)
```

As pointed out in Remark 4, already with the smallest LMI relaxation $d = 2$, we obtain a certificate of global optimality, and a unique global minimizer (truncated at 5 digits): $(k_1,\ k_2,\ k_3) = (9.3786 \cdot 10^{-2},\ 8.6296 \cdot 10^{-2},\ 1.5690 \cdot 10^{-1})$ that corresponds to the second solution in the second block of Table 1 (the "regular" one as expected).

References

[1] N.N. Antoun. *State Space Analysis and Optimization of Marx Generator*. PhD thesis, University of New Mexico, Albuquerque, NM, 2006.

[2] S. Basu, R. Pollack, and M.F. Roy. *Algorithms in real algebraic geometry*. Springer, Berlin, 2006.

[3] D.J. Bates, J.D. Hauenstein, A.J. Sommese, and C.W. Wampler. Software for numerical algebraic geometry: a paradigm and progress towards its implementation. In *Software for algebraic geometry*, volume 148 of *IMA Vol. Math. Appl.*, pages 1–14. Springer, New York, 2008.

[4] A. Ben-Tal and A. Nemirovski. *Lectures on modern convex optimization*. SIAM, Philadelphia, PA, 2001.

[5] H. Bluhm and D. Rusch. *Pulsed power systems*. Springer, Berlin, 2006.

[6] C.J. Buchenauer. Optimizing compact marx generator networks. *IEEE Transactions on Plasma Science*, 38(10):2771–2784, 2010.

[7] W.J. Carey and J.R. Mayes. Marx generator design and performance. In *Twenty-Fifth International Power Modulator Symposium and High-Voltage Workshop*, pages 625–628, Hollywood, CA, 2002.

[8] J.N. Chiasson, L.M. Tolbert, K.J. McKenzie, and Zhong Du. Elimination of harmonics in a multilevel converter using the theory of symmetric polynomials and resultants. *IEEE Transactions on Control Systems Technology*, 13(2):216–223, 2005.

[9] M.T. Chu. Inverse eigenvalue problems. *SIAM Review*, 40(1):1–39, 1998.

[10] M.T. Chu and G.H. Golub. *Inverse eigenvalue problems: theory, algorithms, and applications*. Oxford University Press, New York, 2005.

[11] D. Cox, J. Little, and D. O'Shea. *Ideals, varieties, and algorithms*. Springer, New York, 2007.

[12] A. Eremenko and A. Gabrielov. Counterexamples to pole placement by static output feedback. *Linear Algebra and its Applications*, 351/352:211–218, 2002.

[13] A. Eremenko and A. Gabrielov. Pole placement static output feedback for generic linear systems. *SIAM Journal on Control and Optimization*, 41(1):303–312, 2002.

[14] J.C. Faugère. A new efficient algorithm for computing Gröbner bases (F_4). *Journal of Pure and Applied Algebra*, 139(1-3):61–88, 1999.

[15] J.C. Faugère. A new efficient algorithm for computing Gröbner bases without reduction to zero (F_5). In *Proceedings of the International Symposium on Symbolic and Algebraic Computation*, pages 75–83, 2002.

[16] J.C. Faugère, P. Gianni, D. Lazard, and T. Mora. Efficient computation of zero-dimensional Gröbner basis by change of ordering. *Journal of Symbolic Computation*, 16(4):329–344, 1993.

[17] G.H. Golub and C.F. Van Loan. *Matrix computations*, volume 3. Johns Hopkins University Press, Baltimore, MD, 1996.

[18] T. Gunji, S. Kim, M. Kojima, A. Takeda, K. Fujisawa, and T. Mizutani. PHoM–a polyhedral homotopy continuation method for polynomial systems. *Computing*, 73(1):57–77, 2004.

[19] D. Henrion and J.B. Lasserre. Solving nonconvex optimization problems. *IEEE Control Systems*, 24(3):72–83, 2004.

[20] D. Henrion and J.B. Lasserre. Detecting global optimality and extracting solutions in GloptiPoly. In *Positive polynomials in control*, volume 312 of *Lecture Notes in Control and Inform. Sci.*, pages 293–310. Springer, Berlin, 2005.

[21] D. Henrion, J.B. Lasserre, and J. Löfberg. GloptiPoly 3: moments, optimization and semidefinite programming. *Optimization Methods & Software*, 24(4-5):761–779, 2009.

[22] J.B. Lasserre. Optimisation globale et théorie des moments. *C. R. Acad. Sci. Paris Sér. I Math.*, 331(11):929–934, 2000.

[23] J.B. Lasserre. *Moments, positive polynomials and their applications*. Imperial College Press, London, 2010.

[24] J.B. Lasserre, M. Laurent, and P. Rostalski. Semidefinite characterization and computation of zero-dimensional real radical ideals. *Foundations of Computational Mathematics*, 8(5):607–647, 2008.

[25] M. Laurent. Sums of squares, moment matrices and optimization over polynomials. In *Emerging applications of algebraic geometry*, volume 149 of *IMA Vol. Math. Appl.*, pages 157–270. Springer, New York, 2009.

[26] J. Rosenthal and J. C. Willems. Open problems in the area of pole placement. In *Open problems in mathematical systems and control theory*, Comm. Control Engrg. Ser., pages 181–191. Springer, London, 1999.

[27] F. Rouillier. Solving zero-dimensional systems through the rational univariate representation. *Applicable Algebra in Engineering, Communication and Computing*, 9(5):433–461, 1999.

[28] F. Rouillier and P. Zimmermann. Efficient isolation of polynomial's real roots. *Journal of Computational and Applied Mathematics*, 162(1):33–50, 2004.

[29] F. Sottile. *Real solutions to equations from geometry*. American Mathematical Society, Providence, RI, 2011.

[30] J.F. Sturm. Using SeDuMi 1.02, a MATLAB toolbox for optimization over symmetric cones. *Optimization Methods and Software*, 11/12(1-4):625–653, 1999.

[31] B. Sturmfels. *Solving systems of polynomial equations*. American Mathematical Society, Providence, RI, 2002.

[32] L. N. Trefethen and Mark Embree. *Spectra and pseudospectra: the behavior of nonnormal matrices and operators*. Princeton University Press, Princeton, NJ, 2005.

[33] J. Verschelde. PHCpack: a general-purpose solver for polynomial systems by homotopy continuation. *ACM Transactions on Mathematical Software*, 25(2):251–276, 1999.

[34] X. Wang. Decentralized pole assignment and product Grassmannians. *SIAM Journal on Control and Optimization*, 32(3):855–875, 1994.

[35] L. Zaccarian, S. Galeani, M. Francaviglia, C.T. Abdallah, E. Schamiloglu, and C.J. Buchenauer. A control theory approach on the design of a Marx generator network. In *IEEE Pulsed Power Conference*, Washington, DC, June 2009.